Anal. Chem. **2010,** *82,* 1012–1019

Antimicrobial Susceptibility Testing Using High Surface-to-Volume Ratio Microchannels

Chia Hsiang Chen,[†] Yi Lu,[†] Mandy L. Y. Sin,[†] Kathleen E. Mach,[‡] Donna D. Zhang,[§] Vincent Gau,[||] Joseph C. Liao,[‡] and Pak Kin Wong*[,†,⊥]

Department of Aerospace and Mechanical Engineering, P.O. Box 210119, Department of Pharmacology and Toxicology, University of Arizona, 1703 East Mabel Street, and Biomedical Engineering and Bio5 Institute, University of Arizona, Tucson, Arizona 85721, Department of Urology, Stanford University, 300 Pasteur Drive, S-287, Stanford, California 94305-5118, and GeneFluidics Inc., 2540 Corporate Place, Suite B-101, Monterey Park, California 91754

This study reports the use of microfluidics, which intrinsically has a large surface-to-volume ratio, toward rapid antimicrobial susceptibility testing at the point of care. By observing the growth of uropathogenic *Escherichia coli* in gas permeable polymeric microchannels with different dimensions, we demonstrate that the large surface-to-volume ratio of microfluidic systems facilitates rapid growth of bacteria. For microchannels with 250 μm or less in depth, the effective oxygenation can sustain the growth of *E. coli* to over 10^9 cfu/mL without external agitation or oxygenation, which eliminates the requirement of bulky instrumentation and facilitates rapid bacterial growth for antimicrobial susceptibility testing at the point of care. The applicability of microfluidic rapid antimicrobial susceptibility testing is demonstrated in culture media and in urine with clinical bacterial isolates that have different antimicrobial resistance profiles. The antimicrobial resistance pattern can be determined as rapidly as 2 h compared to days in standard clinical procedures facilitating diagnostics at the point of care.

Antimicrobial susceptibility test (AST) is often performed to determine the antibiotic sensitivity of bacterial pathogens in clinical samples such as urine, blood, sputum, or wound swabs.[1] The current clinical practice requires sample transportation to a centralized microbiology laboratory and overnight culture of the infectious agents. AST results are not available for days after sample collection. These aspects have limited the accessibility at the point of care. Rapid determination of antimicrobial susceptibility is especially crucial toward judicious management of infectious diseases in emergency situations and high-risk areas such as hospitals, intensive care units, and clinics established in response to disasters.[2−4] Without objective information of the drug resistance profile of the suspected pathogen, physicians have to select antibiotic therapy empirically based on the nature of the infection and antibiotic treatments are typically chosen based on the worst-case-scenario assumption. Injudicious use of broad spectrum antibiotics by clinicians, as a result of lack of objective diagnosis at the point of care and significant delay of standard procedures, has contributed to the emergence of resistant pathogens worldwide.[5,6] A point-of-care device for rapid AST in resource limited settings is, therefore, highly desirable. It will lead to evidence-based, rather than empiric, management of infectious diseases and will allow more judicious use of antibiotics, which in turn will reduce the emergence of multidrug-resistant pathogens.[7]

While various genotypic markers have been identified for antibiotic resistance, measurement of the phenotypic response of bacteria to antibiotics is often superior to genotypic detection of antibiotic resistance genes due to the diverse resistance mechanisms and the continuous evolution of the pathogens.[1,8] In particular, growth-based phenotyping AST methods are the current gold standard in clinical microbiology laboratory. Conventional techniques for determining antibiotic resistance include broth dilution and disk diffusion.[9,10] For disk diffusion, the bacterial isolates are inoculated on the surface of an agar plate and a disk-shaped filter paper soaked with a standard amount of antibiotic is loaded onto the surface of the dish. With the diffusion of the antibiotic and the formation of an antibiotic concentration gradient into the adjacent medium, after 18−24 h period of incubation, a zone of inhibition of bacterial growth appears depending on the effectiveness of the antibiotic. The size of the

* To whom correspondence should be addressed. Phone: +1-520-626-2215. Fax: +1-520-621-8191. E-mail: pak@email.arizona.edu.

[†] Department of Aerospace and Mechanical Engineering, University of Arizona.

[‡] Stanford University.

[§] Department of Pharmacology and Toxicology, University of Arizona.

[||] GeneFluidics Inc.

[⊥] Biomedical Engineering and Bio5 Institute, University of Arizona.

(1) Balows, A., Ed. *Current Techniques for Antibiotic Susceptibility Testing*; Thomas: Springfield, IL, 1974.

(2) Liao, J. C.; Mastali, M.; Gau, V.; Suchard, M. A.; Moller, A. K.; Bruckner, D. A.; Babbitt, J. T.; Li, Y.; Gornbein, J.; Landaw, E. M.; McCabe, E. R. B.; Churchill, B. M.; Haake, D. A. *J. Clin. Microbiol.* **2006**, *44*, 561–570.

(3) Fridkin, S. K.; Edwards, J. R.; Tenover, F. C.; Gaynes, R. P.; McGowan, J. E.; Project, I.; Hosp, N. S. *Clin. Infect. Dis.* **2001**, *33*, 324–329.

(4) Kollef, M. H.; Fraser, V. J. *Ann. Intern. Med.* **2001**, *134*, 298–314.

(5) Infectious Disease Society of America Task Force on Antimicrobial Availability, 2004.

(6) Kardas, P.; Devine, S.; Golembesky, A.; Roberts, C. *Int. J. Antimicrob. Agents* **2005**, *26*, 106–113.

(7) Hawkey, P. M. *J. Antimicrob. Chemother.* **2008**, *62*, I1–I9.

(8) Sommer, M. O.; Dantas, G.; Church, G. M. *Science* **2009**, *325*, 1128–1131.

(9) Bauer, A. W.; Kirby, W. M. M.; Sherris, J. C.; Turck, M. *Am. J. Clin. Pathol.* **1966**, *45*, 493.

(10) Stalons, D. R.; Thornsberry, C. *Antimicrob. Agents Chemother.* **1975**, *7*, 15–21.

10.1021/ac9022764
Published on Web 01/07/2010

inhibition zone provides an indication of the potency of the antibiotic and is inversely proportional to the minimum inhibitory concentration.[1] The disk diffusion and agar diffusion methods, while "low-tech" and labor-intensive, are well established and still commonly used, particularly in resource-limited settings. To automate the labor intensive procedures and provide quantitative assessment of the antimicrobial sensitivity, various techniques that directly measure the concentration of the pathogens (e.g., optical density and micromechanical oscillators) or their activities (e.g., microcalorimetry, bioluminescence, and radioactive CO_2 release) have been developed to facilitate the identification and evaluation of the antimicrobial resistance of bacteria in microtiter plates or other formats.[11−16] All the current automated antimicrobial susceptibility techniques rely on first isolating the pathogens from the body fluid or tissue samples, which takes 18−24 h, followed by phenotypic testing of the isolated bacteria for AST, which takes another 18−24 h of incubation. Furthermore, these systems are expensive and have bulky footprints. With the use of a fluorescent viability indicator and an epifluorescence microscope, an emulsion-based microfluidic technique has been recently reported by observing the activity of individual bacteria confined in droplets.[17] AST results can be obtained in 7.5 h. Nevertheless, all these systems are difficult to be adapted to a point-of-care setting. In particular, the major hurdles for these techniques toward rapid, point-of-care testing are the time-consuming bacterial growth step and the requirement of bulky supporting instrumentation.

The advent of microfluidics has the potential to revolutionize the clinical management of infectious diseases and the implementation of AST at the point of care.[18,19] An important requirement for rapid bacterial growth is sufficient oxygen in the microenvironment.[20] In conventional bacteria culture, vigorous shaking with an orbital shaker is typically applied to facilitate oxygenation in the media to sustain the bacterial growth. Oxygenator systems are often included in perfusion circuits and bioreactors to supply adequate oxygen for tissue and cell culture.[21−23] On the other hand, microfluidic devices have intrinsically a large surface-to-volume (S/V) ratio as a result of the small length scale. This provides a simple, yet effective, approach for oxygenation inside a microfluidic cell culture system.[24] At a given concentration of bacteria, the amount of oxygen required for sustaining the bacterial growth is proportional to the volume of the culture media (i.e., number of bacteria) while the oxygen flux is proportional to the surface area. This implies relatively abundant oxygen is available for bacterial culture at the microscale. Figure 1 illustrates the effect of the dimension of the microchannel for bacterial culture. The large S/V ratio of microfluidics for facilitating effective oxygenation has been utilized in various chip-based cell studies.[25−29] Nevertheless, the relationship between the S/V ratio and bacterial growth has not been investigated systematically, and the microfluidic approach has not been demonstrated for rapid AST.

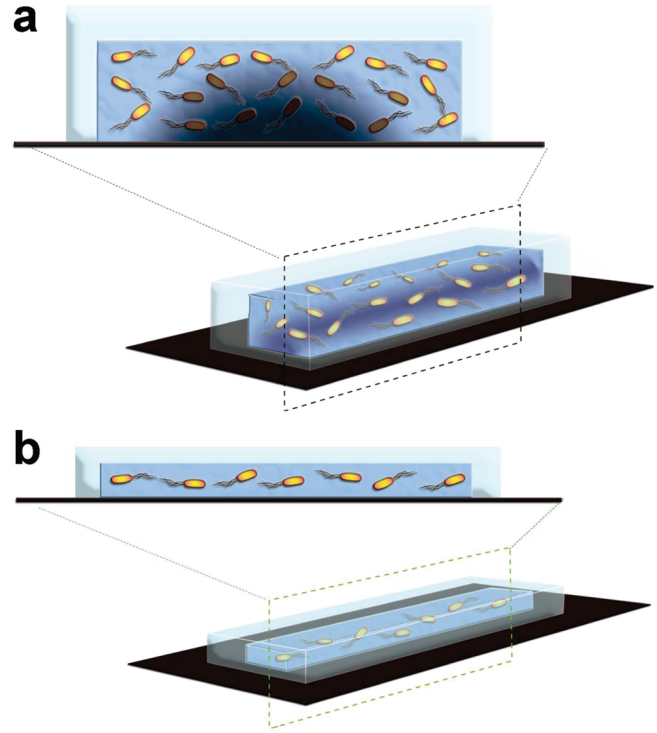

Figure 1. Schematics illustrating the effect of the depth of a microchannel on the growth of *E. coli*. (a) For a microchannel with a large depth, the oxygen level is relatively low for supporting the growth of all *E. coli* as a result of the large S/V ratio. (b) For a microchannel with a small depth, the oxygen level is relatively abundant, which supports rapid growth of the pathogens.

In this study, we explore the use of gas permeable polydimethylsiloxane (PDMS) microchannels that has a large S/V ratio toward the implementation of rapid AST at the point of care. The growth of uropathogenic *Escherichia coli* in microfluidic channels was compared to other culture conditions, including an Erlenmeyer flask in an orbital shaker, a static Erlenmeyer flask, and a static Petri dish. The bacterial growth was investigated as a function of the S/V ratio of the apparatus by using laser-

(11) Ljungholm, K.; Wadso, I.; Mardh, P. A. *J. Gen. Microbiol.* **1976**, *96*, 283–288.
(12) Deblanc, H. J.; Wagner, H. N.; Charache, P. *Antimicrob. Agents Chemother.* **1972**, *22*, 360.
(13) Isenberg, H. D.; Maclowry, J. D. *Annu. Rev. Microbiol.* **1976**, *30*, 483–505.
(14) Gfeller, K. Y.; Nugaeva, N.; Hegner, M. *Biosens. Bioelectron.* **2005**, *21*, 528–533.
(15) Ertl, P.; Robello, E.; Battaglini, F.; Mikkelsen, S. R. *Anal. Chem.* **2000**, *72*, 4957–4964.
(16) Mann, T. S.; Mikkelsen, S. R. *Anal. Chem.* **2008**, *80*, 843–848.
(17) Boedicker, J. Q.; Li, L.; Kline, T. R.; Ismagilov, R. F. *Lab Chip* **2008**, *8*, 1265–1272.
(18) Kim, J.; Junkin, M.; Kim, D. H.; Kwon, S.; Shin, Y. S.; Wong, P. K.; Gale, B. K. *Microfluid. Nanofluid.* **2009**, *7*, 149–167.
(19) Liao, J. C.; Mastali, M.; Li, Y.; Gau, V.; Suchard, M. A.; Babbitt, J.; Gornbein, J.; Landaw, E. M.; McCabe, E. R. B.; Churchill, B. M.; Haake, D. A. *J. Mol. Diagn.* **2007**, *9*, 158–168.
(20) Schulze, K. L.; Lipe, R. S. *Arch. Mikrobiol.* **1964**, *48*, 1-&.
(21) Borenstein, J. T.; Terai, H.; King, K. R.; Weinberg, E. J.; Kaazempur-Mofrad, M. R.; Vacanti, J. P. *Biomed. Microdevices* **2002**, *4*, 167–175.
(22) Knazek, R. A.; Kohler, P. O.; Gullino, P. M.; Dedrick, R. L. *Science* **1972**, *178*, 65.
(23) Maharbiz, M. M.; Holtz, W. J.; Sharifzadeh, S.; Keasling, J. D.; Howe, R. T. *J. Microelectromech. Syst.* **2003**, *12*, 590–599.
(24) Kim, D.-H.; Wong, P. K.; Park, J.; Levchenko, A.; Sun, Y. *Annu. Rev. Biomed. Eng.* **2009**, *11*, 203–233.
(25) Gomez-Sjoberg, R.; Leyrat, A. A.; Pirone, D. M.; Chen, C. S.; Quake, S. R. *Anal. Chem.* **2007**, *79*, 8557–8563.
(26) Balagadde, F. K.; You, L. C.; Hansen, C. L.; Arnold, F. H.; Quake, S. R. *Science* **2005**, *309*, 137–140.
(27) Zanzotto, A.; Szita, N.; Boccazzi, P.; Lessard, P.; Sinskey, A. J.; Jensen, K. F. *Biotechnol. Bioeng.* **2004**, *87*, 243–254.
(28) Wong, P. K.; Yu, F. Q.; Shahangian, A.; Cheng, G. H.; Sun, R.; Ho, C. M. *Proc. Natl. Acad. Sci. U.S.A.* **2008**, *105*, 5105–5110.
(29) Walker, G. M.; Zeringue, H. C.; Beebe, D. J. *Lab Chip* **2004**, *4*, 91–97.

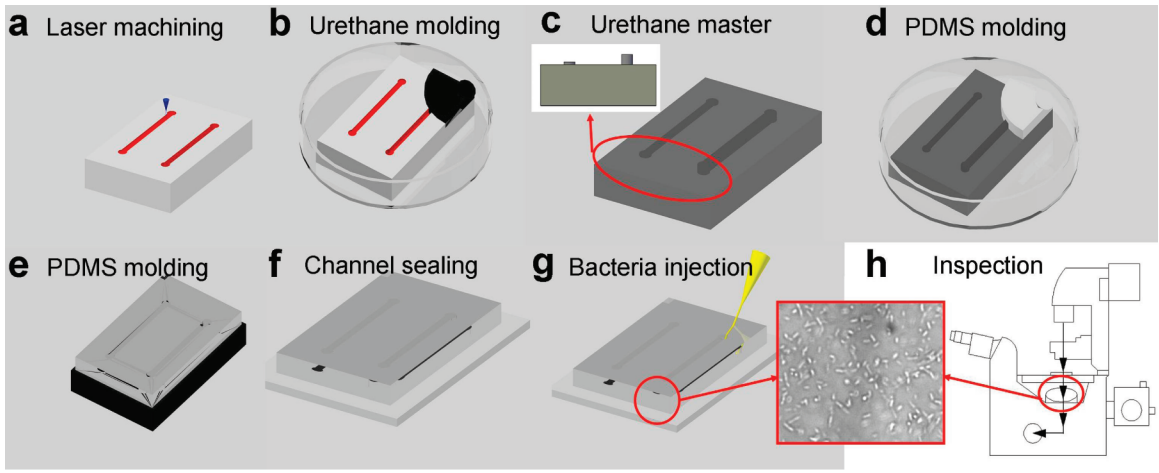

Figure 2. Process flow for fabricating microfluidic channels with different S/V ratios for rapid AST. (a) A CO_2 laser machining system was used to engrave microchannels on a polycarbonate substrate. Different channel depths can be generated simultaneously in the process. (b) Urethane molding on the polycarbonate master. (c) A reverse, urethane mold with microchannels of different depths. Only two channels are shown for simplicity. The insert shows the cross-section view. (d, e) PDMS channels were molded on the urethane mold. (f) The PDMS channel was sealed with a glass substrate using an atmospheric (air) plasma system. The plasma treatment step also sterilized the channel. (g) Injection of pathogens into the channel with a syringe. Microchannels were washed with PBS and incubated with or without BSA before the experiment. (h) Bacterial growths can be monitored by phase contrast microscopy or absorbance spectroscopy.

machined microchannels with different depths. Understanding the effect of the S/V ratio on bacterial growth helps to optimize the microfluidic design for rapid AST. Experimental results are presented to determine the dose dependence of ampicillin on an uropathogenic *E. coli* using microfluidic channels. Furthermore, the antimicrobial resistance profiles of four *E. coli* clinical isolates were also determined using the microfluidic channels with an optimized S/V ratio. These tests can be performed directly in urine mixed with bacteria culture media. The current study will potentially form the technological foundation of a microfluidic approach for performing rapid AST at the point of care without relying on a centralized clinical microbiology laboratory.

EXPERIMENTAL SECTION

Microchannel Fabrication. To evaluate the possibility of rapid bacterial culture using microfluidic channels, we designed microfluidic channels with different depths, which adjust the overall S/V ratio. The channels were fabricated using a combination of laser-micromachining and a two-step polymer molding process. PDMS, which is gas permeable and transparent, was chosen as the channel structural material. PDMS is one of the silicone polymers that has a high oxygen diffusivity.[30] A two-stage molding process was developed to fabricate microchannels with different S/V ratios (Figure 2). Briefly, laser machining was performed to engrave polycarbonate substrates, which served as the master mold of the microchannels. A laser machining system (Versa, Universal Laser System Inc.) was applied, and the cutting depth (i.e., the final channel depth) was controlled by adjusting the laser power and duration. The laser-machined polycarbonate master was characterized using optical microscopy. Channel dimensions on the order of 100 μm can be easily created with this laser machining process. A reverse mold was then created by molding urethane on the polycarbonate master mold overnight at room temperature. After the urethane mold was solidified, it was peeled off and cut to appropriate size for PDMS molding. The PDMS channel layer was cured at 70 °C overnight. The PDMS channel layer and a glass substrate were sterilized and bonded using an atmospheric (air) plasma system. To test the effect of surface coating on bacterial adhesion, the channel was incubated with 1% (w/v) bovine serum albumin (BSA) for 10 min and rinsed with phosphate buffered saline (PBS). Different channel depths can be created on the same mold using this process. The master mold had 12 channels. In this study, microchannels with depth of 114 to 2707 μm were fabricated. For the 200 μm channel, the length and width were 25.4 and 2 mm, respectively. This resulted in a total volume of approximately 10 μL inside the channel.

Bacterial Strains. Uropathogenic *E. coli*, which accounts for more than 80% of uncomplicated urinary tract infection (UTI), was selected as the model pathogen for this study. Four *E. coli* strains (EC137, EC132, EC462, and EC136) isolated from clinical urine samples of patients with UTI were used. These strains were isolated as part of a research protocol approved by the Stanford University Institutional Review Board. For each bacterial strain, four conditions were tested: no antibiotic control, ampicillin (Amp), ciprofloxacin (Cipro), and trimethoprim/sulfamethoxazole (T/S). All three antibiotics chosen are commonly used oral antibiotics for UTI treatment. The four *E. coli* strains have different antimicrobial resistance profiles, which were previously determined by the clinical microbiology laboratory. EC137 is sensitive to all three antibiotics (Amp^S, $Cipro^S$, T/S^S); EC136 is resistant to ampicillin (Amp^R); EC132 is resistant to ampicillin and ciprofloxacin (Amp^R, $Cipro^R$); and EC462 is resistant to ampicillin and trimethoprim/sulfamethoxazole (Amp^R, T/S^R). These clinical isolates were cultured in Mueller-Hinton medium, which is the standard laboratory media for minimum inhibitory concentration (MIC) and AST tests.[31] Before the experiment, bacteria on agar plate were inoculated in Mueller-Hinton medium. The clinical isolates were grown to an early expo-

(30) Charati, S. G.; Stern, S. A. *Macromolecules* **1998**, *31*, 5529–5535.

(31) Atlas, R. M.; Parks, L. C. *Handbook of Microbiological Media*, 2nd ed.; CRC Press: Boca Raton, FL, 1997.

nential phase and diluted to appropriate concentrations for the experiment. *E. coli* strain DH5α was also used in control experiments and was cultured in Lysogeny broth.

Bacterial Growth in Microchannels. The growth of uropathogenic *E. coli* inside a microchannel was compared to other culture conditions. The bacteria samples were injected into 200 μm depth channels by syringes. At the same time, 13 and 5 mL of bacteria samples were pipetted into an Erlenmeyer flask and a 60 mm Petri dish, respectively. The amounts of the solution were chosen that the height of the media is 3 mm in both apparatuses. The flasks, Petri dishes, and microchannels were incubated statically in a miniaturized incubator at 37 °C. One of the flasks was loaded into an orbital shaker (BarnStead Inc.) at 250 rpm and 37 °C as a positive control. For optical inspection, the microfluidic channels were directly mounted on a digital microscope equipped with phase contrast optics (Leica, DMI 4000B). The morphology and density of the bacteria were recorded by a CCD camera (Planetary Imaging, DMK 31AF03) and digitized into a video capture system (Image Source, IC Capture 2.0). The growth of the bacteria was monitored at regular time intervals using a microsample spectrophotometer (Nanodrop 2000) by withdrawing all the solution from the microchannel. The concentration of the bacteria was determined by observing the absorbance at 600 nm. Similar experiments were also performed using *E. coli* DH5α. To determine the effect of the S/V ratio on the bacterial growth rate, the clinical isolate EC137 was injected into channels from 114 to 2707 μm in depth. Different volumes of bacterial samples were also loaded to Erlenmeyer flasks, which resulted in different S/V ratios. The range of S/V ratio spanned from 0.05 to 94.4 cm^{-1} in our experiment. Each condition was repeated at least four times.

Oxygen Supply and Consumption. As PDMS is gas permeable, oxygen can diffuse into the medium inside a microchannel. The order of magnitude of the maximum oxygen flux F_{max} by diffusion through the PDMS layer can be approximated by the diffusion equation:[32]

$$F_{max} = D_{PDMS}\left(\frac{\Delta C}{\Delta z}\right) \quad (1)$$

In eq 1, D_{PDMS}, ΔC, and Δz denote the diffusivity of oxygen in PDMS, the difference of oxygen concentration across the PDMS layer, and the thickness of the PDMS layer, respectively. The diffusivity of oxygen in PDMS[30] is 4.1×10^{-9} m^2/s. The oxygen concentration in the atmosphere is 0.2 mol/m^3 and is used to estimate the maximum oxygen difference.[32] The PDMS thickness Δz is 2 mm for the current microchannel design. If the channel width and length are large compared to the depth, the oxygen supply is dominated by the top surface and is approximately the same for channels with different depths. For a 200 μm depth channel, the total surface area of the gas permeable PDMS channel is 6.18×10^{-5} m^2, and the maximum oxygen flux is estimated to be 25.3 pmol/s. On the other hand, the oxygen consumption rate depends on the particular bacteria being tested. The oxygen consumption rate of *E. coli* has been reported to be 1.78×10^{-18} mol/cell/s.[33] For the same concentration of *E. coli*, a deeper channel requires more oxygen than a shallower channel, as the total number of bacteria is proportional to the volume of the channel. At a bacteria concentration of 1.4×10^9 cfu/mL in a 200 μm channel, the oxygen consumption rate is the same as the maximum oxygen flux of 25.3 pmol/s.

(32) Leclerc, E.; Sakai, Y.; Fujii, T. *Biomed. Microdevices* **2003**, *5*, 109–114.
(33) Geckil, H.; Stark, B. C.; Webster, D. A. *J. Biotechnol.* **2001**, *85*, 57–66.

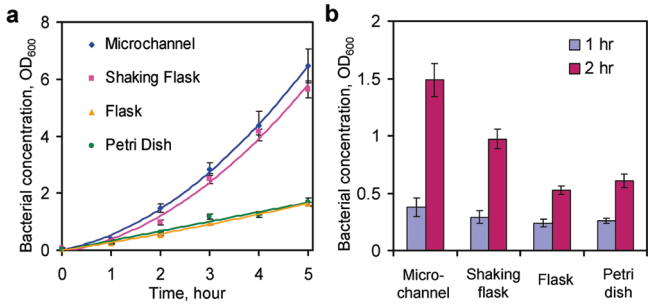

Figure 3. Comparison of bacterial growth in a 200 μm microchannel (microchannel), an Erlenmeyer flask inside a shaking incubator (shaking flask), a static Erlenmeyer flask (flask), and a static Petri dish (Petri dish). (a) The bacterial growth curves for *E. coli* EC137 in different conditions. Bacteria in the shaking flask grew at a similar rate compared to bacteria inside the microchannel. The bacteria in the static flask and Petri dish displayed significantly lower growth rates compared to the microchannel. (b) Initial growth rates were similar after 1 h for all experimental conditions. After 2 h of bacterial culture, the growth rates can be clearly distinguished. Each data point represents at least four experiments. Data represent absorbance ± standard deviation.

Microfluidics Based AST. Experiments were performed to determine the MIC of ampicillin using 200 μm microfluidic channels. The clinical isolate EC137 in Mueller-Hinton medium was used in the experiment. Furthermore, antimicrobial resistance profiling experiments were performed to evaluate the applicability for microfluidic AST. Stock solutions of antibiotics were freshly prepared before each experiment. The concentrations of Amp and Cipro were 100 and 4 μg/mL, respectively. Trimethoprim and sulfamethoxazole were mixed at a 1:19 ratio (16 and 304 μg/mL). These concentrations were selected based on standard AST protocols. Antibiotic samples were prewarmed at 37 °C for 20 min. The antibiotics were then mixed with the clinical isolates and culture media before being injected into microchannels. The experiment was also performed by mixing urine and Mueller-Hinton medium at 1:1 ratio. In addition, *E. coli* DH5α and DH5α transformed with an ampicillin resistance gene were tested using the same procedure. In all AST experiments, microchannels with a depth of 200 μm were incubated at 37 °C for 2 h. The concentrations of bacteria were determined using the Nanodrop spectrophotometer. A pathogen was considered to be sensitive to an antibiotic if the bacterial concentration is less than 30% of the control value.

RESULTS AND DISCUSSION

Effect of S/V Ratio on Bacterial Growth. To evaluate the effectiveness of microfluidic bacteria culture, the growth of bacteria inside a 200 μm microchannel was compared to other apparatuses and culture conditions (Figure 3a). In the first hour, significant growths were observed in all culture conditions. The growth rates were similar initially between all different culturing conditions. As the bacteria continued to grow, the static Petri dish

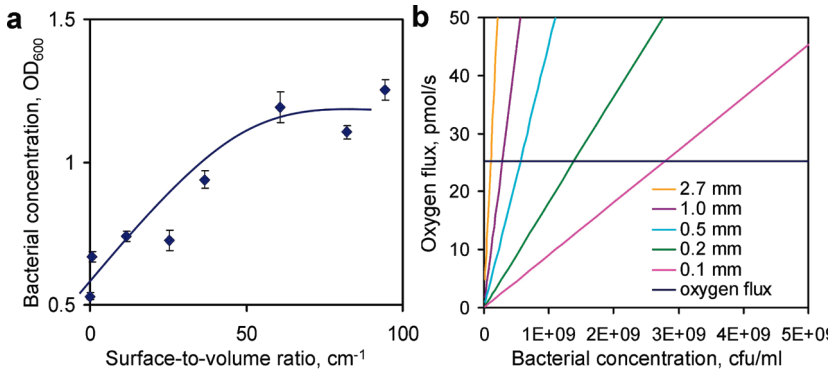

Figure 4. (a) The effect of the S/V ratio on bacterial growth after culturing for 2 h. The bacterial growth increased with the S/V ratio and saturated at approximately 60 cm^{-1} corresponding to a channel of 250 μm in depth. Error bars represent the standard deviation. (b) Comparison of the oxygen consumption rates for different channel depths. The blue line indicates the oxygen supply for the channel used in the experiment.

and flask displayed significantly slower growth rates compared to the microchannel. The growth rates could be clearly distinguished after 2 h. Figure 3b compares the growth of EC137 after 1 and 2 h of bacterial culture. With the use of the microchannel, the absorbance value reached ~1.5 in 2 h while the static dish and flask required 5 h to result in a similar value. The growth rate (i.e., the slope of the growth curve) of the *E. coli* in the microchannel was similar to the value in the shaking flask. A slight delay of the bacterial growth (the growth curve shifted to the right for ~5 min) was consistently observed for the shaking flask when compared to the microchannel (Figure 3a). This can be understood by the difference in thermal time constants of the microchannel and the flask.[34] More importantly, the fast growth rate in the microchannel that is comparable to the shaker flask opens the possibility of eliminating the bulky culture equipment, which dramatically simplifies the system requirement for point-of-care AST. To further evaluate the effect of the S/V ratio on bacterial growth, the clinical isolate EC137 was cultured in channels with different depths. Figure 4a shows the concentration of the bacteria after 2 h of inoculation, and the growth rate generally increased with the S/V ratio. For 2 h of bacterial culture, the absorbance value appeared to saturate when the S/V ratio was equal to or greater than 60 cm^{-1}. This S/V ratio was corresponding to a microchannel with a depth of 250 μm. Further increase in the S/V ratio (i.e., channels with smaller depths) showed little effect on the growth of the bacteria. The same result was also observed using *E. coli* DH5α (data not shown).

An order-of-magnitude calculation has been performed to estimate the oxygen supply and consumption during bacterial culture inside a microfluidic channel. Figure 4b compares the oxygen consumption rates for different channels, which is proportional to the volume of the channel and the concentration of the bacteria. If the surface area is fixed at 6.18×10^{-5} m^2, the maximum oxygen flux is approximately 25.3 pmol/s. For a 200 μm channel, the maximum oxygen flux coincides with the oxygen consumption rate at a concentration of 1.4×10^9 cfu/mL. For a channel with a smaller depth (e.g., 100 μm channel), the curve intersects with the oxygen flux at a higher absorbance value ($\sim 2.8 \times 10^9$ cfu/mL). Oxygen will become limited for bacterial growth near the intersection points. For a channel with a larger depth, the interaction point occurs at a much lower bacterial concentration. The channel with 1 mm depth has 5 times more bacteria than the 200 μm channel; therefore, it consumes 5 times more oxygen.

In general, our results indicate that the S/V ratio plays an important role in the bacterial growth and that a microchannel with a large S/V ratio can facilitate rapid bacterial growth. The experimental observations can be understood by considering the oxygen available to the bacteria in the microchannel. For an apparatus with a small S/V ratio (e.g., the static flask and Petri dish), the oxygen flux is only enough to support the growth of the bacteria at low concentration. This was likely to be the case during the first hour of bacteria culture when the bacterial concentration was relatively low. Indeed, the observed growth rates were similar in the first hour when the bacterial concentrations were relative low in different culture conditions. At a higher bacteria concentration, the oxygen was insufficient for sustaining the growth of the bacteria and the bacteria displayed slower growth rates in the static flask and Petri dish after 2 h of inoculation (Figure 3). For an apparatus with a large S/V ratio, an excessive amount of oxygen is available for the bacteria and bacterial growth. This provides an explanation for the maximum absorbance value observed after 2 h of inoculation (Figure 4a). In this condition, further reduction of the channel depth could not improve the bacterial growth. As demonstrated in our data, a microchannel with 250 μm or less in depth sustained the growth of *E. coli* to over 10^9 cfu/mL. This value is in good agreement with our order of magnitude estimation considering the oxygen consumption rate inside the channel and the bacterial growth rate generally correlates with the oxygen supply and the S/V ratio of the apparatus.

In addition to effective oxygenation, the large S/V ratio could also result in other effects. For instance, the bacteria can adhere to the surface of the microchannel, which may affect its growth rate. For PDMS microchannel, the surface is known to promote bacteria adhesion. In order to reduce bacterial adhesion on the channel surface, BSA was incubated in the channel and Figure 5 shows bacterial adhesion on the surfaces of 200 μm depth channels with and without BSA coating after 2 h of inoculation. A significant amount of *E. coli* was attached to the surface while the BSA coating significantly reduced the adhesion (Figure 5). Nevertheless, the values cannot be distinguished based on the

(34) Figliola, R. S.; Beasley, D. E. *Theory and Design for Mechanical Measurements*, 4th ed.; John Wiley: Hoboken, NJ, 2006.

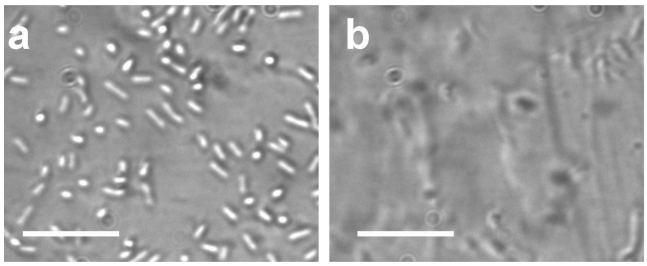

Figure 5. The effect of BSA coating on bacteria adhesion: (a) bacteria adhesion on the channel surface without BSA coating and (b) the number of *E. coli* adhered to the surface can be reduced with 10 min incubation of BSA prior to the experiment. Images were taken after 4 h of bacterial culture and removal of the suspension. Scale bars represent 20 μm.

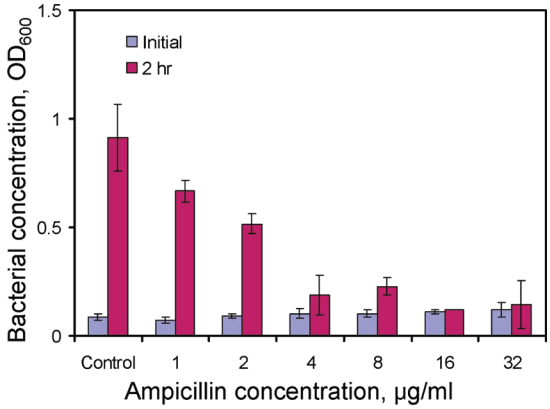

Figure 6. Minimum inhibitory concentration (MIC) determination using microchannels. The MIC of ampicillin to EC137 was determined using high S/V ratio microchannels. The growth of the bacteria was observed to be insignificant at concentration higher than 4 μg/mL. The experiments were performed in Mueller-Hinton broth. Data represent mean $\pm$ standard deviation.

absorbance measurement. This is likely due to the fact that the number of bacteria adhered on the surface is relatively small compared to the bacteria in suspension. This shows that bacterial adhesion has an insignificant effect on the measurement in the current experimental condition. The volume of the sample is another consideration for optimizing the S/V ratio especially at a low pathogen concentration. At low concentration (e.g., less than 10 bacteria in the channel), random variation of the initial number of bacteria could introduce uncertainty in the measurement. If necessary, the channel length and width should be increased to obtain a large volume of sample while maintaining the S/V ratio by adjusting the depth of the channel. Additionally, extra incubation time can be applied in microfluidic AST to eliminate the uncertainty due to the variation in the initial concentration. On the basis of these results and considerations, a channel depth of 200 μm was designed in all the successive AST experiments and the culture time was chosen to be 2 h.

Dose Dependence of Antibiotics. The parallel processing nature of microfluidics provides a useful tool for performing multiplexed tests simultaneously. For instance, we have determined the dose dependence of ampicillin for the uropathogenic *E. coli* EC137 using microfluidic channels. The pathogens were inoculated with different concentrations of ampicillin inside the microchannels. Figure 6 shows the result of the dose dependence test using 200 μm microfluidic channels. Without ampicillin, the bacteria grow to an optical density over 1 within 2 h. At a lower concentration (e.g., 1 or 2 μg/mL), a slight decrease in the bacterial grow was observed compared to the control. Nevertheless, the concentration of the pathogen was significant compared to the control (over 50%). At an ampicillin concentration equal to or greater than 4 μg/mL, the growth of the bacteria was less than 30% of the control value. Total inhibition of the bacterial was observed at 16 μg/mL or higher. This suggests the lowest concentration of ampicillin to inhibit the growth of the *E. coli* ES 137 is 16 μL.

Antimicrobial Resistance Profiling of Clinical Isolates. Antimicrobial resistance profiling is required to determine the antibiotic susceptibility pattern of a pathogen. This provides clinically relevant information for selecting the type of antibotic that a patient will receive. To demonstrate the applicability of microfluidic devices for AST, we cultured four *E. coli* clinical isolates in four different conditions (no antibiotics, Amp, Cipri, and T/S) and observed their growths after 2 h. Figure 7a shows the result of microfluidic AST in Mueller-Hinton media. The absorbance value of the control set for EC137 strain is 1.4, and the value is significantly higher than other conditions with antibiotics. This indicates that the EC137 strain is sensitive to these antibiotics. EC132, which is sensitive to T/S and resistant to Amp and Cipro, displayed significant growth with Amp and Cipro but insignificant growth with T/S compared to the control. The antibiotic resistance profiles of the EC462 and EC136 strains were also determined. These results agree with the antibiotic resistance profiles previously determined by the clinical microbiology laboratory. Therefore, the antimicrobial resistance profiles of all these four clinical isolates were determined successfully using microfluidic AST in 2 h. To explore the feasibility of directly performing microfluidic AST in biological fluids, similar experiments were also performed by mixing the culture media with the pathogens in urine (Figure 7b). Interestingly, we observed faster growth rates of the uropathogens in urine mixed with culture media (except EC462). The absorbance of EC132 in urine was almost twice of the value in culture media. We also observed a larger variation in the bacterial growth with the antibiotics in urine. Nevertheless, the antibiotic resistance profiles for all four clinical isolates were correctly identified using microfluidic AST. This supports that the microfluidic AST approach can be directly applied for AST of uropathogens in urine. In addition, we have also demonstrated rapid AST using standard laboratory strain *E. coli* DH5α genetically engineered with and without ampicillin resistance (data not shown). Together, our data demonstrate the general applicability of using microfluidics for rapid AST and the approach is compatible with urine and potentially other biological fluids.

In this study, we investigated the effect of the S/V ratio to bacterial growth using laser-machined microchannels with different dimensions. Our data suggest that microchannels with 250 μm or less in depth can provide sufficient oxygen for the growth of uropathogenic *E. coli* to over 10^9 cfu/mL. The experimental observation is in good agreement with the order-of-magnitude calculation based on oxygen balance. The value is also consistent with a previous bioreactor study, which reports that a reactor depth of 300 μm can support the growth of 10^9 cfu/mL.[27] It should be noted that this value depends on the

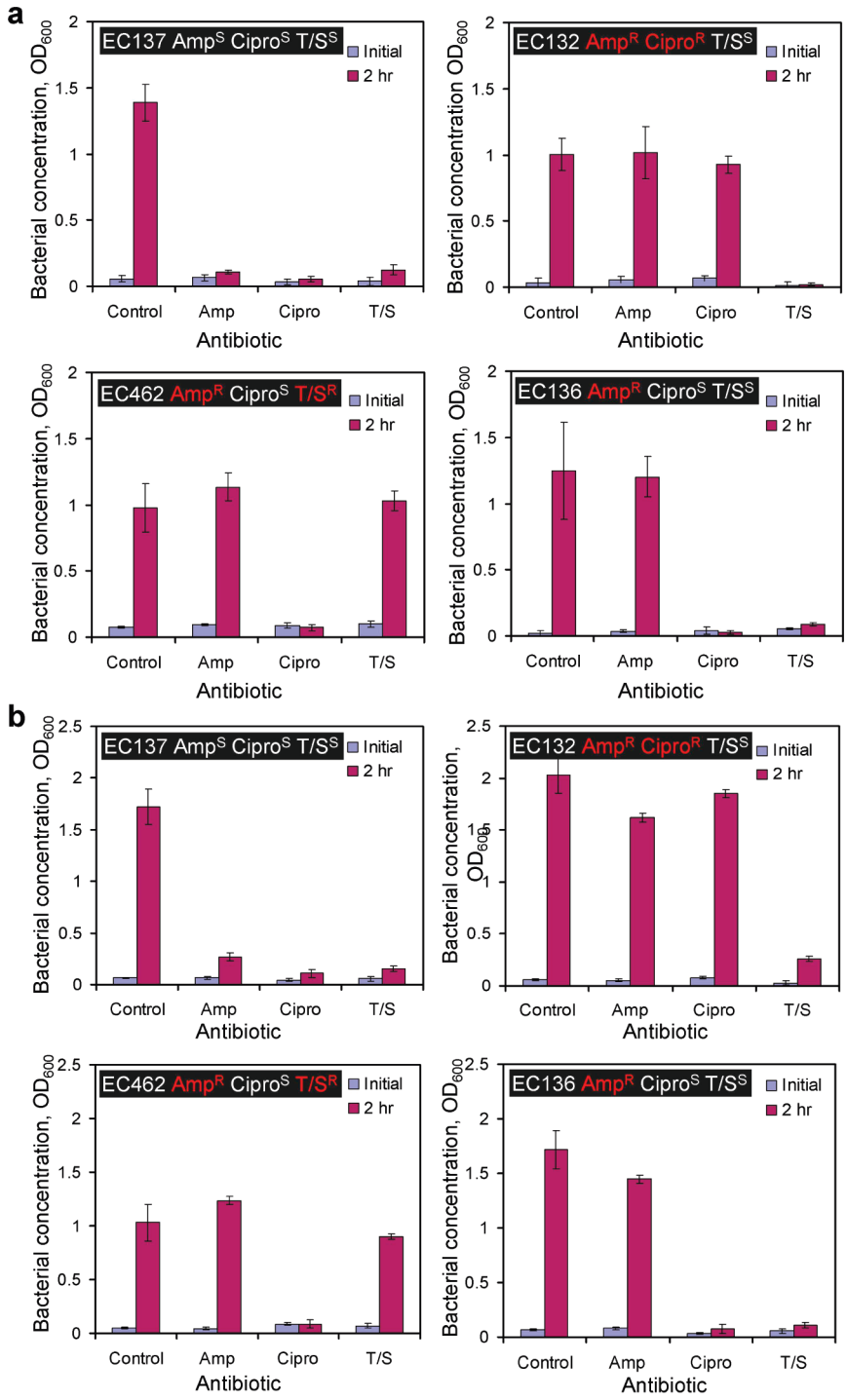

Figure 7. Antimicrobial susceptibility testing (AST) using microchannels: (a) four clinical isolates (EC137, EC132, EC462, and EC136) were tested for their antimicrobial resistance patterns in Mueller-Hinton media. The antimicrobial resistance patterns for ampicillin (Amp), ciprofloxacin (Cipro), and trimethoprim/sulfamethoxazole (T/S) of the strains are highlighted in the figure. The superscripts "S" and "R" indicate sensitive and resistance of the strain to the antibiotics. (b) Antimicrobial resistance profiling of the same clinical isolates in urine using 200 μm microchannels. The experiments were performed in Mueller-Hinton media mixed with urine at a 1:1 ratio. Data represent mean $\pm$ standard deviation.

particular strain of pathogens. In general, our results will serve as guidelines for optimizing the channel design for rapid AST. For instance, the PDMS thickness and channel depth can be further reduced to facilitate oxygen transportation if necessary. The bottom substrate can also be replaced by gas permeable materials to further increase the surface area. Another major finding in this study is that microfluidic AST can be finished in a 2 h time frame, which is 1−2 orders of magnitude faster than the standard AST procedures currently in clinical practice. The reported plug-based stochastic confinement technique, which is not optimized by oxygen transportation, requires 7 h for MIC determination and AST.[17] Furthermore, we have shown that the microfluidic AST technique is directly applicable to urine. This may potentially simplify the labor-intensity and time-consuming sample preparation steps in the AST procedure and facilitates point-of-care AST in nontraditional settings. In

addition, the microfluidic approach offers several other advantages for rapid AST at the point of care. First, the microfluidic platform can be easily integrated with other detection systems for monitoring the growth of the bacteria. For instance, microelectrode arrays can be easily deposited on the glass substrate for performing microscale impedimetric analysis[35,36] or electrochemical sensing.[2,19,37,38] On-chip monitoring of the bacterial activity may improve the accuracy of the assay by eliminating the uncertainty due to the lag phase of the bacteria. Second, various microfluidic techniques, such as surface modification,[39,40] gradient generation,[41,42] and electrokinetic manipulation,[43,44] can be combined to enhance the functionality of the system for automated AST and other drug screening applications.

(35) Yang, L. J. *Talanta* **2008**, *74*, 1621–1629.
(36) Cheng, X.; Liu, Y. S.; Irimia, D.; Demirci, U.; Yang, L. J.; Zamir, L.; Rodriguez, W. R.; Toner, M.; Bashir, R. *Lab Chip* **2007**, *7*, 746–755.
(37) Gau, V.; Ma, S. C.; Wang, H.; Tsukuda, J.; Kibler, J.; Haake, D. A. *Methods* **2005**, *37*, 73–83.
(38) Mach, K. E.; Du, C. B.; Phull, H.; Haake, D. A.; Shih, M. C.; Baron, E. J.; Liao, J. C. *J. Urol.* **2009**, *182*, 2735–2741.
(39) Keyes, J.; Junkin, M.; Cappello, J.; Wu, X.; Wong, P. K. *Appl. Phys. Lett.* **2008**, *93*, 023120.
(40) Junkin, M.; Watson, J.; Geest, J. P. V.; Wong, P. K. *Adv. Mater.* **2009**, *21*, 1247–1251.
(41) Jeon, N. L.; Dertinger, S. K. W.; Chiu, D. T.; Choi, I. S.; Stroock, A. D.; Whitesides, G. M. *Langmuir* **2000**, *16*, 8311–8316.
(42) Irimia, D.; Geba, D. A.; Toner, M. *Anal. Chem.* **2006**, *78*, 3472–3477.
(43) Wong, P. K.; Chen, C. Y.; Wang, T. H.; Ho, C. M. *Anal. Chem.* **2004**, *76*, 6908–6914.
(44) Sin, M. L. Y.; Shimabukuro, Y.; Wong, P. K. *Nanotechnology* **2009**, *20*, 165701.

CONCLUSIONS

We have demonstrated a microfluidic device for bacterial culture and rapid AST in resource limited settings. The large S/V ratio of microfluidic systems facilitates effective oxygenation for bacterial culture and provides a simple and effective platform for rapid AST at the point of care. The microfluidic approach allows antimicrobial resistance profiling to be finished as rapidly as 2 h. In the future, high S/V ratio microchannels can be combined with other detection and microfluidic strategies to enhance the functionality of the system. We envision that the microfluidic, point-of-care AST system will improve the clinical management of infectious diseases by allowing more judicious use of antibiotics, which reduces the emergence of multidrug-resistant pathogens.

ACKNOWLEDGMENT

The authors thank Dr. Zheng Sun for valuable discussion. This work is supported by NIH NIAID (Grant 1U01AI082457), NSF ECCS (Grant 0900899), and VA RR&D Merit Review (Grant B4872) awarded to J.C.L.

Received for review October 8, 2009. Accepted December 20, 2009.

AC9022764